Plant and Soil **206:** 61–77, 1999.

The root zone dynamics of water uptake by a mature apple tree

Steve Green* and Brent Clothier
Environment and Risk Management Group HortResearch Institute Private Bag 11-030 Palmerston North New Zealand

Received 12 May 1998. Accepted in revised form 29 September 1998

Key words: sap-flow, time-domain reflectometry (TDR), transpiration, soil water, modelling

Abstract

We report the results from a field experiment in which we examined the spatial and temporal patterns of water uptake by a mature apple tree (*Malus domestica* Borkh., 'Splendour') in an orchard. Time Domain Reflectometry (TDR) was used to measure changes in the soil's volumetric water content, and heat-pulse was used to monitor locally the rates of sap flow in the trunk and roots of the tree. We also measured the tree's distribution of root-length density and obtained supporting data to characterize the soil's hydraulic properties. The experimental data were used to examine the output of the WAVE-model (Vanclooster et al, 1995; Ecol. Model. 81, 183–185) in which soil water transport is predicted using Richards' equation, and where root uptake is represented by a distributed macroscopic sink term.

When the surface soil layers were uniformly wet, 70% of the trees water uptake occurred in the top 0.4 m of the root zone, in which approximately 70% of the tree's fine roots were located. When a partial irrigation was applied to just one side of the root zone, the apple tree quickly shifted its pattern of water uptake with an almost two-fold increase in uptake from the wetter soil parts and a corresponding reduction in uptake from the drier parts. The response of root-sap flow to irrigation was almost immediate (i.e. root flow increased within hours of the irrigation). Following subsequent irrigations over the whole soil surface, TDR measurements revealed a surface-ward shift in the pattern of water extraction, and root flow measurements revealed a recovery in the uptake function of seemingly inactive roots located in the previously-dry soil. Via our root sap flow measurements, we observed two roots on the same tree locally responding quite differently to similar events of soil wetting. This observation suggests that there may be considerable functional variability across the apple root system. Our measurement-model calculations yielded similar results and stress the prime role played by the plant in modifying the root zone balance of water. Following an irrigation or rainfall event, root uptake by apple appears to be more dependent upon the near-surface availability of water than it is related to the distribution of fine roots.

Introduction

Water is essential for all living plants. It is the vehicle that carries nutrients, such as fertilizer, from the surface through the soil to the roots and it is the medium through which other transport processes (i.e. diffusion) take place. With both fertigation and the more traditional methods of fertilizer application, the practical goal is to maintain adequate water and nutrients within the root zone. For environmental protection, it is meanwhile imperative that percolation losses of water and chemical below the root zone are minimized. If application rates or methods are poorly matched to either the soil type, or the plant's requirements, surface-applied chemicals that are water-borne may eventually bypass the root zone, and proceed onward to pollute the groundwater.

Understanding the physical processes in the soil which govern water and chemical entry into the root zone, is a necessary step towards developing more efficient and environmentally sustainable strategies of root zone management. However, it is also important to understand the biological processes that operate in

* FAX No: 6 354-6731. E-mail: greens@hort.cri.nz

the root zone to govern subsequent uptake of water and chemicals by the roots. The movement of soil water, and of any water-borne chemicals, is frequently a direct result of the action of plant roots. If we are to understand better, and to model effectively, soil and plant processes we need at least a quantitative means of describing the process of uptake by the roots. This is particularly true if we are to predict the fate of any surface-applied water and chemicals because roots are the 'big movers' in soil (Clothier and Green, 1997). First, however, we must obtain better observations of these uptake processes and how they are affected by the water and nutrient status of root zone environment.

In this paper we present some measurements of water uptake by mature apple trees growing in an orchard. We compare these measurements against predictions from a deterministic model of the soil water dynamics and root uptake. Data to test the model were obtained from a field experiment in which we monitored directly the rates of transpiration and water uptake by an apple tree. Both soil-based and plant-based observations were used. We also measured the tree's distribution of fine roots (diameter < 2 mm) and obtained data to characterize the soil's hydraulic properties. We use the comparison between measured and predicted patterns of water uptake by roots to illustrate the prime role played by the plant in establishing the water balance of the root zone.

Materials and methods

Theory

Hughes and Gandar (1993) observed that the root systems of mature apple trees, say of age greater than about 10 yrs, have fully overlapped with that of the neighbouring trees. Thus, the root distribution varies predominantly with depth, and has only a minor variation with radial distance from the tree stem. As we show later, our soil coring broadly supports this contention for the apple tree used in this experiment. Here we consider the tree root system as a distributed sink, and we approximate the depthwise distribution of roots using a simple 1-D formulation.

For the purpose of modelling, we use the WAVE-model of Vanclooster et al. (1995). Soil water transport is predicted using the Richards' equation and root uptake is represented by a macroscopic sink term, $S(z)$, viz.

$$C(h)\frac{\partial h}{\partial t} = \frac{\partial}{\partial z}\left[K(h)\left(\frac{\partial h}{\partial t} + 1\right)\right] - S(z). \qquad (1)$$

Here h is the soil water pressure head [m], t is time [s], z is the vertical depth [m] taken as positive downwards, $K(h)$ is the hydraulic conductivity [m s^{-1}], and $C(h) = \mathrm{d}\theta/\mathrm{d}h$ is the soil water capacity function [m^{-1}]. An expression for $C(h)$ can be derived from the soil's moisture retention curve, $\theta(h)$. In order to predict the transient flow of water using Equation (1), constitutive relations describing the soil's hydraulic properties, namely for $K(h)$ and $\theta(h)$, plus the macroscopic sink term describing water uptake, namely $S(z)$, must be known, or approximated.

We will ignore any effects that hysteresis (Mualem, 1974) and preferential flow (Gerke and Van Geneuchten, 1993) might have on the soil's hydraulic conductivity function and the moisture retention characteristic. The soil's hydraulic conductivity is modeled using the power function proposed by Gardner (1958):

$$K(h) = \frac{K_\mathrm{s}}{1 + (b|h|)^N} \qquad (2)$$

where K_S is the saturated hydraulic conductivity value and b and N are soil-dependent parameters. The soil's moisture retention curve, $\theta(h)$, is modeled using the power function of Van Genuchten (1980):

$$\theta(h) = \theta_\mathrm{r} + \frac{\theta_s - \theta_\mathrm{r}}{(1 + (a|h|)^n)^m} \qquad (3)$$

where θ_s is the saturated soil water content (m^3 m^{-3}), θ_r is the residual soil water content (m^3 m^{-3}), a is the inverse of the air entry value (m^{-1}) and m and n are soil-dependent parameters obtained by fitting Equation 3 to simultaneously measured moisture content and pressure head data.

Modeling water uptake by roots

Water uptake by plant roots is a complex process, determined by interacting physical and physiological processes in the soil-root system. A variety of models have been proposed for root uptake (Gardner, 1991; Molz, 1981). These models usually include a quantitative description of the effective root distribution, with some dependence on soil water potential. WAVE uses the simple approach of Feddes et al. (1978) in which the depthwise pattern of root uptake is given by

$$S(z, h) = \alpha(h) S_\mathrm{m}(z) \qquad (4)$$

where $S_\mathrm{m}(z)$ is the maximum uptake rate (day^{-1}) and

$\alpha(h)$ is a dimensionless function which reduces the actual extraction rate depending on soil water potential. The influence of $\alpha(h)$ is to 'force' the model to reduce uptake from the drier parts of the root zone. For simplicity, and because we have no data to show otherwise, we assume the same $\alpha(h)$ function proposed by Feddes et al. (1978). Optimum water uptake [$\alpha(h)$=1.0] extends from h= −0.1 m to -10.0 m, and there is a linear decrease from saturation down to -0.1 m and from -10.0 m down to the wilting point (h=-150.0 m).

We also assume $S_m(z)$ to be proportional to root length density (Gardner, 1964) and we impose the condition that total daily water uptake by the plant root system must equal the total daily transpiration, E (mm day^{-1}), namely

$$E = \int_0^{Z_r} S(z, h)\mathrm{d}z \tag{5}$$

where Z_r is the total depth of the root zone (m). In other words, we use a known value of E to define the total water uptake, and the measured profile of root length density to distribute this uptake over the depth of the root zone.

Calculation of canopy transpiration

Total transpiration from the apple tree was estimated using a modified version of the Penman-Monteith equation. For this calculation, the total leaf area of the tree was first divided into a fraction of sunlit leaves and a complementary fraction of shaded leaves. Uniform leaf properties were then assumed for each class of leaves (Green, 1993; Sinclair et al., 1976). Since apple leaves are hypostomatous we used the equation

$$\lambda E_P = \sum_i a_i \left[\frac{s R_{n,i} r_{b,i} + \rho c_p D_a}{(s + 2\gamma) r_{b,i} + \gamma r_{s,i}} \right] \tag{6}$$

following Jarvis and McNaughton (1986). In this equation, the summation is made over a set of i uniform leaves each being a fraction, a_i, of the total leaf plan area and having an associated leaf stomatal and boundary layer resistance equal to $r_{s,i}$ and $r_{b,i}$ (s m^{-1}), respectively. E_P represents the total transpiration flux (kg m^{-2} s^{-1}) from all the leaves, $R_{n,i}$ is the net radiation flux density (W m^{-2}) of the ith set of leaves, D_a is the ambient vapour pressure deficit of the air (Pa), λ is the latent heat of vaporisation of water (J kg^{-1}), s is the slope of the saturation vapour pressure curve (Pa K^{-1}) considered uniform throughout the tree, γ is the psychrometric constant (Pa K^{-1}), ρ is the air density (kg m^{-3}), and c_p is the specific heat capacity of air (J kg^{-1} K^{-1}).

The model of Thorpe et al. (1980) was used to calculate a mean leaf stomatal resistance for the sunlit and shaded leaves, viz.

$$r_s = r_m \left(\frac{1 + \beta / R_{p,l}}{1 - \delta D_a} \right) \tag{7}$$

where $R_{p,l}$ is the incident photosynthetic photon flux density on the leaf surface (μmol m^{-2} s^{-1}), r_m is the minimum resistance (s m^{-1}), and δ and β are empirical coefficients. We assumed $R_{p,l}$ for the sunlit leaves was equal to half the incoming global radiation, $R_{p,g}/2$, while the corresponding value for the shaded leaves was set equal to 0.1 times this value, as was found to be consistent with the light levels recorded by the photon sensor mounted on top of the porometer (Green and McNaughton, 1997). Values for the other parameters were assumed the same as suggested for apple leaves by Thorpe et al. (1980).

Leaf boundary layer resistances, r_b, were calculated from the empirical relation derived by Landsberg and Powell (1973) which accounts for the mutual sheltering of clustered leaves as:

$$r_b = 58 p^{0.56} (d/U)^{0.5} \tag{8}$$

where d is a characteristic leaf dimension (m), and U is the mean wind speed (m s^{-1}) across the leaf surface which we assume is the wind speed at mean canopy level. The parameter p is a measure of the foliage density 'seen' by the wind, being the ratio of total leaf plan area to the area of foliage projected onto a vertical plane. We assumed equal boundary layer resistance for the sunlit and shade leaves.

Experimental site and plant material

The experiment was carried out in the Massey University research orchard near Palmerston North, New Zealand (lat. 40.2 S, long. 175.4 E), over a 10 week period throughout the summer of 1995. The site and the experimental set up are the same as described by Green et al. (1997). The soil is a Manawatu fine sandy loam consisting of about 0.4 m of sandy loam underlain by about 0.4 m of fine sand, with a gravelly coarse sand beyond about 0.8 m. The experimental data of Clothier et al. (1977) were used for the hydraulic conductivity and water retention characteristics in each

Table 1. Parameters describing the hydraulic characteristics of the Manawatu soil, determined by fitting Equations (2) and (3) to the water retention and hydraulic conductivity data of Clothier et al. (1977). FSL is a fine sandy loam; FS is a fine sand; and GCS is a gravely coarse sand

Depth [m]	Texture	θ_s [%]	θ_r [%]	α [m^{-1}]	n	m	K_s [m day^{-1}]	b [mm^{-1}]	N
0–0.4	FSL	39.0	5.2	23	1.01	1.0	0.55	1.13	1.33
0.4–0.8	FS	37.0	8.7	177	2.33	1.0	2.51	0.14	1.34
> 0.8	GCS	27.0	8.8	568	2.23	1.0	7.84	0.16	4.13

soil layer, as described by Equations (2) and (3), respectively. The fitted parameters are given in Table 1.

Two trees were selected from the middle of a block of similar-sized apple trees (*Malus domestica* Borkh., 'Splendour') planted at a tree spacing of 3 m in rows which were 4.5 m apart. Each tree was about 14 years old and had been pruned as a central leader, with a crown height of about 5 m, and a crown width of about 3 m. The ground beneath one tree was covered with a low rainout shelter made from waterproof plastic sheets. This prevented all rainfall and unwanted irrigation water from entering the root zone. We refer to this tree as the 'covered' tree. The soil surface surrounding the neighbouring 'control' tree was left uncovered and its root zone remained well-watered, both by irrigation and rainfall throughout the experiment.

The total leaf area of the covered tree, A_T, was measured at the end of the experiment by removing all leaves and passing a subsample (10% by weight) through a Licor leaf area meter. The total leaf area was 29.5 m^2. The area of sunlit leaves, A_L was estimated from the ground shadow area, A_S, during the middle part of the day: this shadow area was 7.5 m^2. As a first approximation we assumed a spherical leaf angle distribution, giving rise to a sunlit leaf area twice as large as the vertical projection on the ground. Thus, of the 29.5 m^2 of total leaf area, some 15 m^2 of leaf were considered to be sunlit with the remaining 14.5 m^2 of leaf considered to be in the shade. For the purpose of calculating transpiration from the apple tree via Equation 6, we assumed the fraction of sunlit and shade leaves remained constant throughout the day, as based on previous light-interception measurements in similar-sized apple trees (Green and McNaughton, 1997).

A trench of 3 m by 3 m had been dug around the covered tree, to a depth of 1.2 m, some six months before the experiment was begun. The purpose of the trench was to isolate and limit the horizontal extent of the root zone. The trench was lined with a 10 mm thick plywood wall and then backfilled with soil on the outside of the trench wall. Prior to the start of the experiment we carefully excavated a small hole near the base of the tree trunk to expose partially three surface roots at a depth of 0.1 m and a distance of about 0.3 m

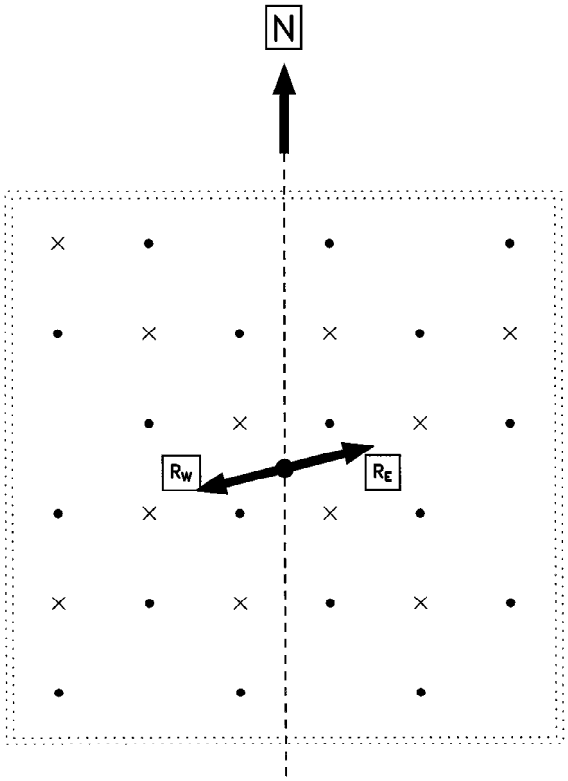

Figure 1. Location of the TDR probes installed vertically into the root zone of the covered tree. There are three TDR probes at each location: (●) marks the location of TDR probes of length 0.1, 0.2 and 0.4 m while (x) shows the probes of length 0.6, 0.8 and 1.0 m. The arrows R_W and R_E indicate the direction of two surface roots emanating from the west and east sides of the tree stem respectively.

from the tree stem. Here we report measurements from just two of these roots which emanated from opposite sides of the tree trunk (Figure 1). One root was on the west side (R_W) and had a diameter of 21 mm while the other root was on the east side (R_E) and had a diameter of 38 mm. Heat pulse probes were installed to monitor sap flow in these two roots. The soil was then carefully repacked around the probes.

Sap flow in the trunk and roots

Sap flow in both the tree stem and the roots was measured routinely using the compensation heat-pulse technique (Green and Clothier, 1988; Swanson and Whitfield, 1981). In the trunk, two sets of probes, each consisting of a heater of 1.8 mm dia. and two temperature probes also of 1.8 mm dia., were installed into parallel holes drilled radially into the tree stem at heights of about 0.5 m above the ground. Sap velocity was measured at radial depths of 5, 12, 20, and 35 mm following the procedure given by Green and Clothier (1988), and using the theoretical calibrations of Swanson and Whitfield (1981) to account for the probe-induced effects of wounding. Volume flow rates, E_H [L/hr], were calculated in the tree stem by integrating the radial profile of sap velocity over the sapwood cross-section.

We used the same procedure to measure root sap flow except that we used smaller size probes to accommodate the smaller diameter of the apple roots. As described by Green et al. (1997), the root probes were only 1.0 mm in diameter and had three sensors equally spaced at depths of between 3.0 to 8.0 mm. A Campbell CR10 data logger (Campbell Scientific Ltd., Logan, Utah, USA) was used to take the heat-pulse measurements once every 20 min.

Spatial pattern of root-water uptake

The soil's volumetric water content (θ) was measured using a digital TDR (Tektronix Model 1502B, Beaverton, Oregon, USA). The TDR measurements were made routinely, every 1–2 days, and the temporal change in the depthwise pattern of θ over periods of almost two weeks were used to deduce the spatial pattern of water uptake by the roots of the covered tree. A laptop computer was used to control the TDR and to record and analyse the TDR waveforms. Analysis of the waveforms followed a procedure similar to that of Baker and Allmaras (1990), using the general equation of Topp et al. (1980) to calculate θ, which we had shown to be appropriate (Vogeler et al., 1997).

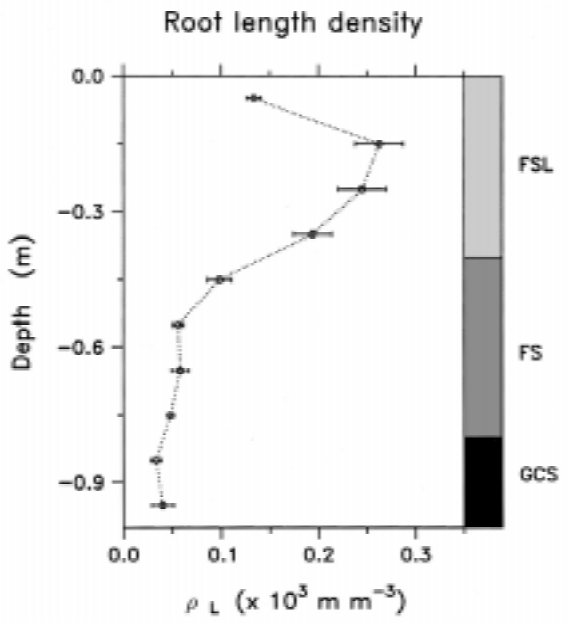

Figure 2. Depthwise profile of mean root-length density, ρ_L (cm cm^{-3}), as determined from the root coring data. The error bars represent ± one standard error about the mean. The shaded boxes show the depths of the three different soil types which comprise the soil profile. FSL = fine sandy loam; FS = fine sand; GCS = gravely coarse sand.

A total of 90 waveguides were installed vertically into the soil around the covered tree (Figure 1). Each waveguide comprised three, parallel stainless-steel rods which were manually connected in sequence to the TDR via a 5 m coaxial cable. The shortest waveguides, of 0.1 m length, were made from stainless-steel rods of 2 mm dia., with a spacing of 25 mm between the two outer rods. All the other waveguides, of 0.2 m length, were made from 6 mm dia. stainless-steel rods, with a distance of 100 mm between the outer two rods.

The waveguides were installed in groups of three, arranged at different radial distances from the tree stem (Figure 1). Probes of length 0.1, 0.2 and 0.4 m were installed at 18 locations while probes of length 0.6, 0.8 and 1.0 m were installed at another 12 locations. A depthwise profile of θ was subsequently obtained by 'differencing' θ-values from adjacent probes.

Root-length density measurements

The distribution of root-length density was measured to compare the patterns of water uptake with the distribution of fine roots (dia. < 2 mm). Soil cores were taken from around the covered tree at the end of the

experiment, using a soil-coring apparatus based on the design of Welbank and Williams (1968). Coring tubes were driven into the ground to a depth of 1.0 m, using a modified concrete breaker. The cores were then extracted using a tripod and winch. A total of 36 cores were taken on a 6 by 6 square grid coinciding approximately with the location of the TDR probes (Figure 1). Each core was sectioned into 100 mm lengths so that a total of 360 core samples were obtained from the root zone. Positions of the core samples were recorded using horizontal distance from the stem and depth to the midpoint of each sample. Roots were then washed from these cores, within a day of sampling, using a commercial root-washing machine (Gillison's Variety Fabrication, Benzie, Michigan, USA). Total root lengths of fine roots, less than 2 mm diameter, were measured using an automatic root-length scanner (Commonwealth Aircraft Corporation Ltd, Melbourne, Australia). The root length density, ρ_l (m m^{-3}), of each sample was determined by dividing the total root length by the core volume. The depthwise distribution of fine roots is shown in Figure 2, as determined from the average of ρ_l at each sample depth within the root zone.

Meteorological measurements

A meteorological station installed close to the experimental tree recorded twenty-minute averages of incoming radiation, wind speed, air temperature, and relative humidity using a Campbell CR10 data logger. The incoming streams of net radiation, R_n (W m^{-2}), and global shortwave radiation, R_s (W m^{-2}), were measured respectively with a Radiation Energy Balance Systems Q*6 net radiometer (Seattle, Washington, USA) and a silicon-cell pyranometer (model PY2100, Licor Ltd., Lincoln, Nebraska, USA). These instruments were mounted on a mast in the middle of the orchard block, at a height of about 2 m above the tree tops and well above any shadows cast by the orchard trees. Air temperature and relative humidity were measured with a Campbell 207 probe, and wind speed was measured with a sensitive 3-cup anemometer. These instruments were mounted on the same mast at a height of about 2.5 m above the ground. This was about mid-canopy level. Vapour pressure deficit of the air, D_a, was computed using the average air temperature and the relative humidity.

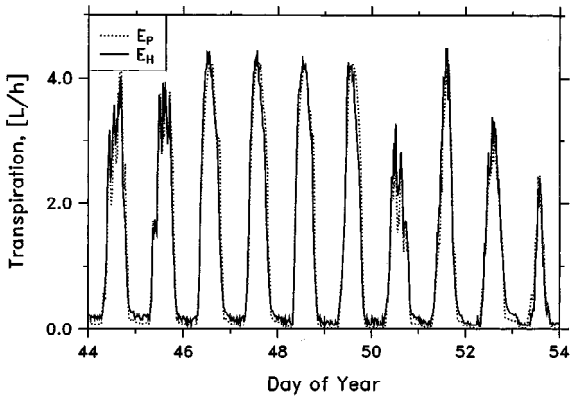

Figure 3. Time course of transpiration in a 14–year–old apple tree during mid summer. E_H is the measured sap flow and E_P is the corresponding rate of transpiration calculated using the Penman-Monteith model.

Irrigation regime

Both the apple trees were thoroughly watered before the start of the experiment. A rainout shelter was installed around the covered tree on 4 February 1995, day-of-year (DOY) 35. The covered tree was subsequently irrigated just four times during the experiment using a purpose-built minisprinkler system. The first irrigation was on DOY 60 when 30 mm of water was used to wet just one half of the soil surface area. This water was applied uniformly to the west side of the tree, to soil occupied by root R_W (Figure 1). After a further two weeks, a second irrigation of about 30 mm was applied uniformly to both sides of the tree. This second irrigation occurred on DOY 76. Subsequent irrigations of about 20 and 80 mm were applied over the whole of the surface soil layer on DOY 87 and 103. The experiment was terminated on DOY 110.

Results

Calculated transpiration from a well-watered tree

Transpiration rates peaked at just over 4 L h^{-1} on warm sunny days (e.g., DOY 46-48). These were reduced to just over 2 L h^{-1} on cloudy, cool days (e.g., DOY 53) due to a reduced atmospheric demand for water (Figure 3). The daily patterns of water uptake displayed, as expected, very little transpiration at night, because the stomata of apple leaves are almost closed in the dark. Throughout the experiment the sap flow measurements remained in good agreement with

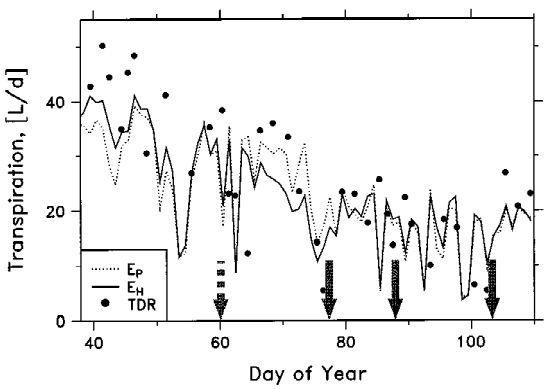

Figure 4. Daily rates of tree water use as calculated by the Penman-Monteith method (broken line) and measured both by TDR (●) and heat-pulse (solid line). The TDR data are averages calculated every 2 to 3 days.

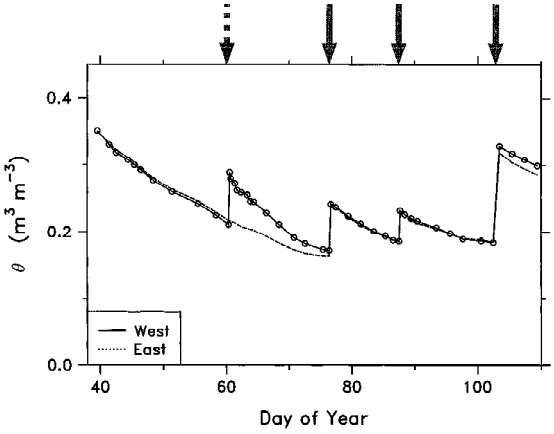

Figure 5. Time course of average soil water content in the top 0.4 m of the root zone, as measured by nine TDR probes on the west (solid line) and east (dotted line) side of the root zone. The locations of these surface probes are shown as the (●) symbol in Figure 1.

the independent calculations of transpiration determined using the Penman-Monteith model. This result gives us added confidence that the calculation procedure of Equation (6) is adequate for the purpose of calculating the diurnal pattern of transpiration from our apple tree. In addition, because sap flow in the covered tree remained similar to that recorded in the neighbouring control tree (data not shown) which was well-watered, it appears unlikely that the covered tree was under any water stress during the experiment. Hereafter, we present only results from the covered tree.

Daily rates of tree water use

The total volume of water being drawn each day from the root zone of the apple tree can be calculated from an integration of the sap flow measurements. Figure 4 shows the results of a calculation of daily transpiration, over each 24 h period starting at midnight. These results are also compared with the corresponding daily changes in soil water content of root zone, as measured by the average of the twelve 1.0 m long TDR probes.

The maximum water use of the apple tree exceeded 40 L day^{-1} in mid-summer (e.g. DOY 40) and thereafter it declined to around 20 L day^{-1} during mid-autumn. This decline is due to a reducing atmospheric demand for water, plus an increasing frequency of rain later in the season.

The three independent estimates of tree water use are very similar, except perhaps during the first 2 weeks of the experiment when the soil-based measurement was between 4 to 15 L day^{-1} higher than both the heat-pulse and the Penman-Monteith calculations (Figure 4). We attribute this discrepancy to surface evaporation of the recently wetted surface soil layers, despite the use of covers to minimise this effect, and some gravity drainage of water beyond the depth of our TDR probes. A difference (or loss) of 15 L day^{-1}, when taken over the soil surface area of 9 m^2, equates to a surface flux of only 1.7 mm day^{-1} which is well below the maximum, 'flux-limited' soil evaporation rate of about 3.0 mm day^{-1} expected for the Manawatu fine sandy loam (Kerr, 1974). Later, we calculate drainage rates and show them to be important only in the first 2 weeks of the experiment.

Changes in water content of the surface soil layers

The depthwise pattern of water uptake can be deduced from the rate at which soil water content changes within different parts of the root zone. However, such a calculation is not altogether straightforward, because any changes in water content reflect not only the water uptake by the plant, but also surface evaporation, plus the addition of water to the root zone following irrigation, and any percolation through it. In this experiment the soil surface was covered, to reduce surface evaporation and exclude rain water, and only measured amounts of irrigation were applied in order to simplify the 'water balance'. Thus, in the absence of significant drainage through the soil profile, the changes in soil water content that we observe should approximately mimic the depthwise pattern of root uptake.

We will first focus our attention on the top 0.4 m of the root zone, since this is the layer of fine sandy loam

Table 2. Change in soil water content as measured by TDR. DOY refers to the day of year, θ [%] is the soil's volumetric water content, z [m] is the depth, and t [day] is the time. $\Delta\theta_1$ is the temporal change in average water content over the soil depths 0–0.4 m, $\Delta\theta_2$ is the corresponding value over the depths 0.0 to 1.0 m, and the subscripts E and W refer to the east and west sides of the root zone. E_H is total stem sap flow recorded by heat-pulse.

DOY	$\int \Delta\theta_{1E}\,dz$	$\int \Delta\theta_{1W}\,dz$	$\int \Delta\theta_{2E}\,dz$	$\int \Delta\theta_{2W}\,dz$	$\int E_H\,dt$
	[L]	[L]	[L]	[L]	[L]
39–60	240	253	392	413	658
60–76	95	209	172	242	359
76–87	103	99	123	90	205
87–102	75	86	104	82	224
103–109	60	53	68	73	113
DOY	$\int \Delta\theta_{1E}\,dz/\int E_H\,dt$	$\int \Delta\theta_{1W}\,dz/\int E_H\,dt$	$\int \Delta\theta_{1}\,dz/\int E_H\,dt$	$\int \Delta\theta_{2}\,dz/\int E_H\,dt$	
39–60	0.36	0.39	0.75	1.22	
60–76	0.26	0.58	0.85	1.15	
76–87	0.50	0.48	0.98	1.04	
87–102	0.33	0.38	0.72	0.83	
103–109	0.53	0.47	1.00	1.25	

where most of the fine roots are located (see Figure 2). For the first three weeks of the experiment, the water content of the top 0.4 m of the root zone dropped rapidly from about 0.35 $m^3\ m^{-3}$ down to 0.21 $m^3\ m^{-3}$ (Figure 5). This reduction in θ of some 14% V/V represents about 500 L of water being withdrawn from the upper part of the root zone (i.e. 14% of the volume of 0.4 m depth times 9 m^2 surface area equates to 500 L). Thus, on average, the water uptake from the top 0–0.4 m of the root zone is 24 L per day, which is about 3/4 of the trees total water uptake over the three-week period (Table 2). We note that approximately 70% of the tree's total length of fine roots were located in the top 0.4 m of the root zone (Figure 2). Thus, water uptake would appear to be in proportion to the total length of fine roots, at least for the case of uniformly wet surface soil layers.

Throughout most of the experiment we observed a similar rate of change in the average water content on both sides of the root zone (Figure 5 and Table 2). This result suggests that root uptake was similar on both sides of the tree, presumably because of similar soil water contents and similar root-length densities. However, this balanced pattern of water uptake was altered for a few weeks following the differential irrigation of just the west side, which occurred on DOY 60. Following the differential irrigation, water uptake from the irrigated, west side of the tree increased relative to the uptake from the drier, east side of the tree (Figure 5). The water content of the west side dropped from about 0.29 down to about 0.17 $m^3\ m^{-3}$ over a period of 16 days. This represents a water loss of some 11% V/V, and is equivalent to about 210 L of water taken up from the top 0.4 m of the root zone (Table 2). A total of 416 L of water was lost from the root zone over the same time period. Thus more than half of the trees water uptake occurred in the top 0.4 m of the wetter, west side of the root zone. In contrast, the corresponding change in soil water on the drier east side of the root zone was about half that value. The remainder of the tree's water uptake was from deeper in the soil profile. These observations provide clear evidence that an apple tree can change significantly its water uptake strategy in response to different levels of soil water availability across the root zone. This observation is consistent with our earlier observations from kiwifruit vines growing on the same Manawatu soil (Green and Clothier, 1995).

Root sap flow following irrigation.

We next examine the heat-pulse measurements of root sap flow to deduce just how quickly the apple tree was able to modify its strategy for water uptake, to take best advantage of irrigation, or rain water. For the purpose of comparison, Figure 6 shows instantaneous

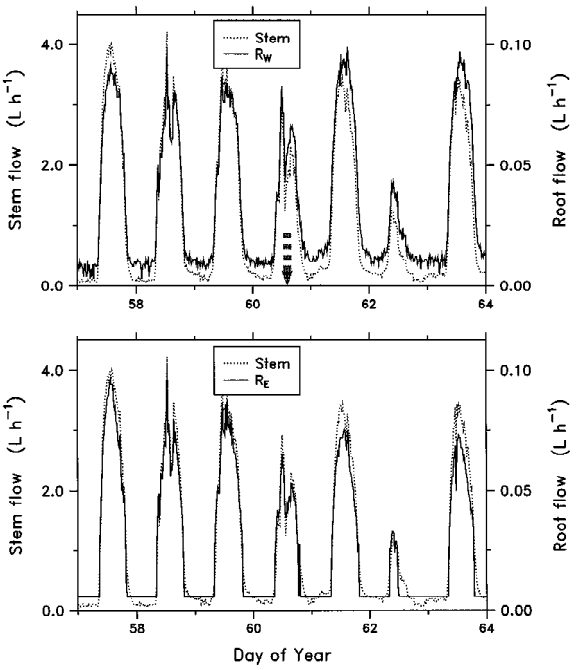

Figure 6. Time course in sap flow measured in the stem and in two surface roots of the apple tree. A partial irrigation of some 30 mm was applied to the west side of the tree, to soil containing root R_W. This irrigation occurred during the middle part of DOY 60, as indicated by the arrow. The soil on the east side of the tree, which contained root R_E, was not irrigated.

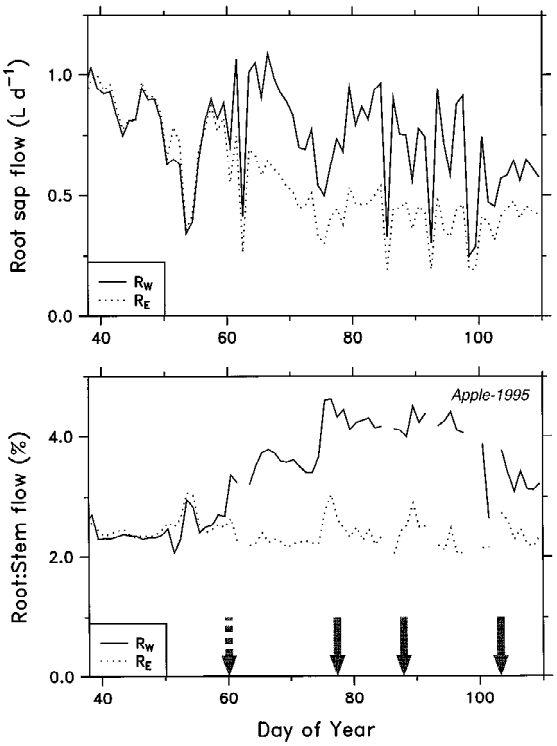

Figure 7. Daily rates of root sap flow following irrigation of the root zone. The arrows indicate the timing of irrigations: A partial irrigation was applied to root R_W on DOY 60. The subsequent irrigations were applied to both roots R_W and R_E (see text for details).

rates of sap flow in the stem, and in two large roots of the apple tree, as recorded once every 20 min by heat-pulse.

The diurnal pattern of root sap flow remained in phase with, and was always similar to the corresponding pattern of sap flow in the tree stem (Figure 6). However, a quite subtle change in root uptake activity did occur when the differential irrigation was applied. Prior to the irrigation, each root was contributing approximately 2.5% of the total stem flow (Figure 6). Following the differential irrigation, sap flow in the wetted root (R_W) increased straight away to be more than 2.8% of stem flow and there was a compensatory decline in sap flow in root R_E. The contribution from this 'dry' root fell to just 2.1% of stem flow. Interestingly, after the differential irrigation was applied, sap flow in the 'wet' root remained elevated in the early evening, for at least one hour longer than did the sap flow in both the stem and the 'dry' root.

In Figure 6, we see the total sap flow in both roots is quite similar, with peak values reaching about 0.1 L h^{-1}. However, the corresponding sap flux-densities in the two roots were very different because root R_W was only about 1/2 the diameter of root R_E. Root R_W had a maximum sap flux density equal to about 0.1 mm s^{-1}, and this is similar to values reported for apple (Cabibel and Do, 1991), kiwifruit (Green and Clothier, 1995) and olive (Moreno et al., 1996) trees. The corresponding sap flux density in the bigger root, R_E, reached a maximum of just 0.03 mm s^{-1}. While we are unable to explain the difference in sap flux densities of the two roots, we suspect the reason could be related to root age (bigger roots may be older and have a lower hydraulic conductivity), or it could be related to root location (root R_E appeared to be heading much deeper into the soil) or root density (the effective root length of R_E may have been less than root R_W).

The daily rates of root sap flow are shown in the top panel of Figure 7, with the ratio of root:stem flow being shown in the bottom panel of the same figure. Daily sap flow in root R_E was about 1.0 L day^{-1} in mid-summer (e.g. DOY 40) and thereafter declined to around 0.5 L day^{-1} by mid-autumn. The corresponding daily sap flow in root R_W also peaked at about 1.0 L day^{-1}. These rates seem reasonable since there were

many large woody roots emanating from the base of the tree stem. The seasonal decline in the sap flow of root R_E was similar to the decline in stem sap flow. Therefore, the ratio of root:stem flow remained reasonably steady, at around the 2.5% level, during the 80 days of the experiment. While root R_E did exhibit small increases in relative flow shortly after each irrigation event, these increases did not last more than just a few days. In contrast, there appeared to be a long-term irrigation response by root R_W which was markedly different to that of root R_E.

The differential irrigation on DOY 60, and the subsequent irrigation to both sides of the vine on DOY 76, each resulted in a large and sustained increase in the sap flow of root R_W which was not observed in the other root R_E (Figure 6). We are unable to explain why root R_E, which resided in previously dry soil, did not exhibit the large a surge in uptake activity following this rewetting that we saw in root R_W when it was first irrigated on DOY 60. We do know that root R_E appeared to have gone deeper into the soil than did root R_W. We speculate that R_E's network of fine roots would have been less able to take advantage of the surface-applied irrigation water, at least until it percolated to depth.

The relative uptake of root R_W, as expressed by the ratio of root:sap flow, increased from 2.5% before irrigation to about 3.5% after the first irrigation and reached almost 4.5% after the second irrigation. While subsequent irrigations saw this ratio drop back to about 3.0% by the end of the experiment, the uptake activity of root R_W was still higher than it had been at the beginning of the experiment. We consider that possible reasons for the enhanced activity of root R_W may have been root signalling, or some growth of new root tips in response to the differential irrigation. Currently, we have no data to confirm this.

Notwithstanding the declining seasonal water use, the heat-pulse measurements of root sap flow provide further experimental evidence that root uptake activity changes significantly in response to different levels of water availability across the root zone.

Changing water content throughout the root zone

We now use TDR observations of the changing pattern of soil water content to illustrate how the depthwise pattern of water uptake from the soil responded to irrigation. We also compare measured patterns of water uptake against the corresponding distribution of fine roots, as measured by root coring at the end of the experiment. We thereby deduce the correspondence between water uptake and root-length density.

Figures 8–10 show the spatial pattern of the average rate of change in soil water content for a seven to ten day period following a full-irrigation, a part-irrigation, and a further full-irrigation of the root zone. Data for these figures were obtained by 'differencing' the average water contents measured by pairs of neighbouring TDR probes of different length. For this analysis we waited for a period of four days after each irrigation, to allow time for the applied water to percolate through the soil profile. We thereafter calculated the subsequent changes in soil water content up until the next irrigation, and attributed these changes as root uptake.

Over the first dry-down period, most of the water uptake occurred within a lateral radius of about 1.2 m from the tree trunk (Figure 8). Uptake was largely confined to the top 0.4 m of the root zone, in a rather 'flat-bowl' shaped region which was broadly consistent with the spatial pattern of fine roots. While the density of fine roots was greatest in the top 0.4 m, the maximum root-length densities were located beyond a radius of 1.0 m (Figure 11). We can speculate that some of these roots could have been 'old' roots from the neighbouring trees, though we have no way of confirming this. Very little uptake occurred beyond a depth of 0.6 m, with water contents there changing by less than about 0.2% V/V per day. This change is small compared to the average water uptake from the surface soil layers, which exceeded 0.65% V/V per day (Figure 8).

Following the differential irrigation of 30 mm to the west side of the tree, we see a preferential uptake of water from the wetted soil, and concomitantly a much reduced uptake of water from dry soil, despite there being no local change in water content there (Figure 9). Water content change from the wetted soil exceeded 0.80% V/V per day while the corresponding uptake from the dry side was almost everywhere less than 0.50% V/V per day. Once again, little uptake occurred beyond a depth of 0.6 m. These soil based measurements of Figure 9 are consistent with the plant based measurements of Figure 6. They both show that uptake activity changed in response to different levels of available soil water and that near-surface roots are most active following rewetting. Clearly, root uptake declined in the dry soil, and this decline was enhanced when there were other regions of the root zone that contained more readily-available water (Figure 9).

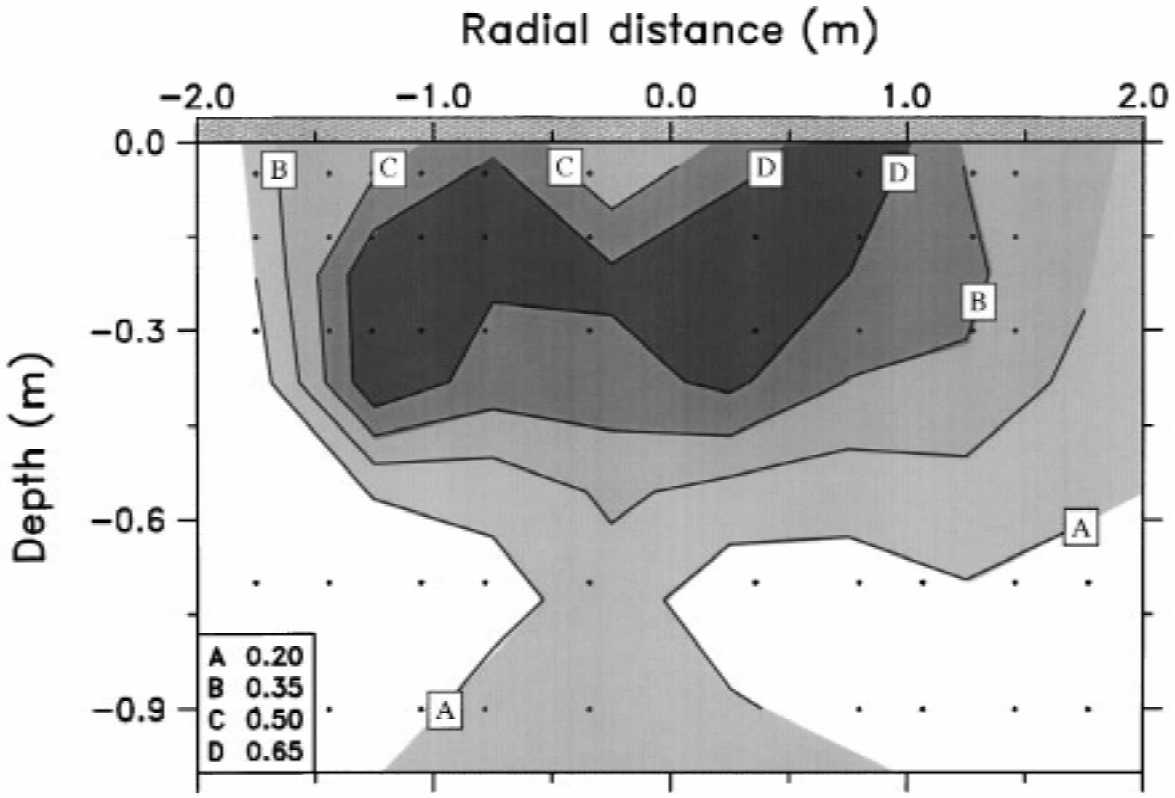

Figure 8. Measurement by TDR of the spatial pattern of the average water uptake, $\Delta\theta$ (% per day) by the covered tree during the initial dry-down period between DOY 48 and 60. The location of each TDR measurement is shown by (●). Irrigation is indicated by the shaded region at the soil surface.

Following the rewetting of both sides of the root zone, on DOY 77, water uptake from the previously dry soil returned to a level similar to that observed in the previously wet soil (Figure 10). We also note that, following this full irrigation, the pattern of uptake more closely matched the distribution of fine roots (Figure 2). This result confirms a recovery in the root function of previously dry roots, which was also seen in the measurements of root sap flow (Green et al., 1997). The correspondence between root-length density and the spatial pattern of water uptake also bodes well for modelling the water uptake process, at least when there is no significant heteorogeneity in the spatial pattern of soil water content.

Modelling

Our TDR observations of soil water content indicate root uptake by an apple tree to be a multi-dimensional, time-dependent process, influenced by a myriad of interacting plant and soil factors. In other words, the process of water uptake is complex and 3-dimensional. Nevertheless, we believe there is merit in attempting to describe such a complex process using a simple conceptual model, e.g. Equation (4), along with a 1-dimensional framework to approximate the root system. So, to round off our experiment, and as a first attempt at modelling soil water movement in the root zone of orchard trees, we sought to investigate whether the WAVE model (Vanclooster et al., 1995) could reproduce the depthwise pattern of water content that we observed using TDR in the root zone of our apple tree. The model-measurement comparison is shown in Figure 12. For the purpose of comparison we have to ignore the period between DOY 60 and 77, because this coincides with the timing of the differential irrigation to just the west side of the root zone. During this period, the WAVE model is not appropriate, because it treats both sides of the root zone as being the same. But, for times other than when the differential irrigation was applied, the model output is appropriate and, indeed, it reproduces a reasonable prediction of the temporal change in soil water of the root zone. We

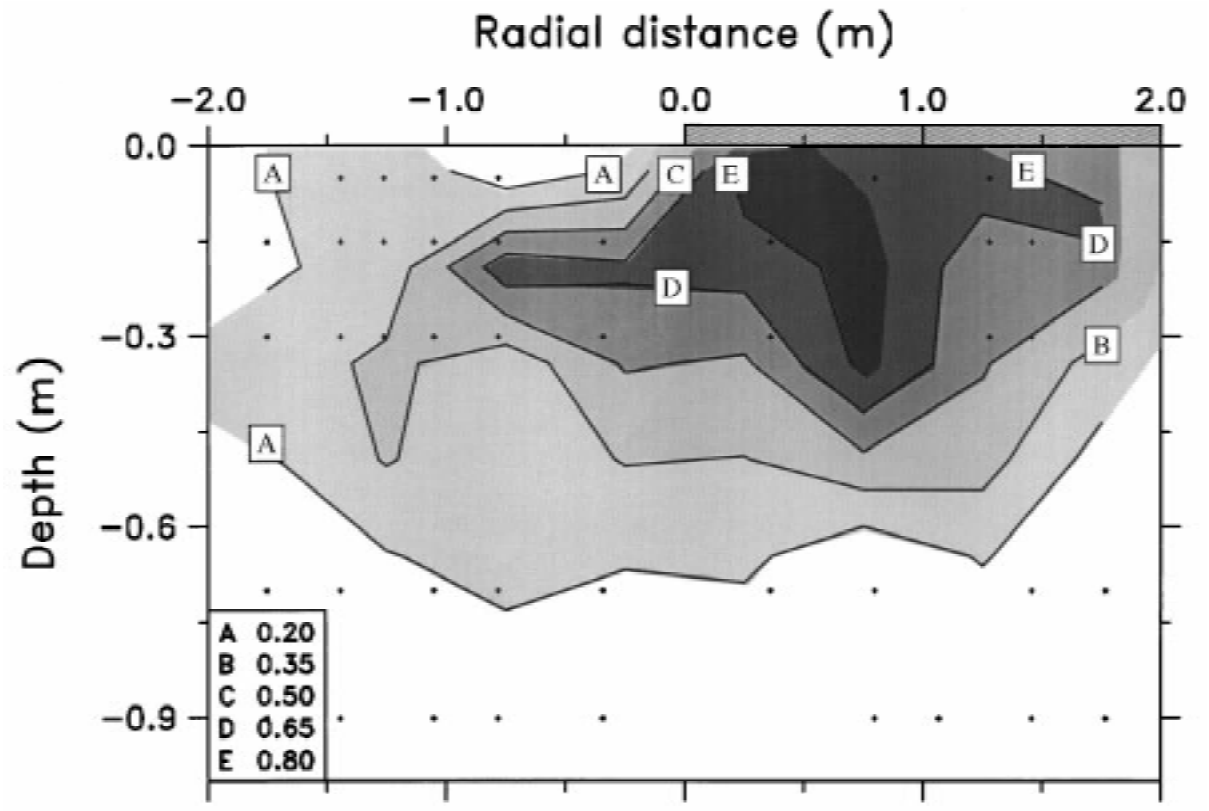

Figure 9. Measurement by TDR of the spatial pattern of water uptake, $\Delta\theta$ (% per day) by the covered tree for the period between DOY 64 and 76, which follows a partial irrigation of some 30 mm to the west side of the tree on DOY 60. Irrigation is indicated by the shaded region at the soil surface.

note that during our experiment the tree had sufficient water in the root zone so there was no reduction in uptake via the $\alpha(h)$ function.

The changing temporal pattern of θ in the different layers of the root zone, as measured by the TDR, reflects the combined influence of water uptake plus any drainage through the soil profile (Figure 12). Immediately following each irrigation large increases in θ are observed in the top layers of the root zone, with smaller changes being observed deeper in the profile. Thereafter, the θ values drop more rapidly in the surface soil layers. This is where more roots are located. A more gradual decline in θ is observed at depth, where there are fewer roots and where the soil water contents are lower.

It is difficult to determine from Figure 12 alone exactly what fraction of the change in θ is due to uptake by the roots, and what fraction is due to drainage. In fact, $d\theta/dt=0$ could represent uptake at depth by roots, balanced by water percolating downwards. Models do offer the possibility of resolving this conundrum by their distinct representation of each process: drainage from a knowledge of $K(h)$, $\theta(h)$ and dh/dz,plus uptake from E, θ and root length density. The simple model of root uptake employed in WAVE, with extraction being proportional to root-length density, yet constrained to the correct total E, generates a reasonable result when compared to the observed patterns of θ (Figure 12). It appears to give the right rates of uptake from the surface soil layers (0–10 cm) as well as from deeper in the profile (40–60 cm), and it also predicts quite well the timing of the drainage to depth. This agreement gives us some confidence in the model of soil water flow, or we are equally wrong for compensating reasons.

The model results allow us to estimate a water balance for the root zone, expressed as the cumulative total of storage, transpiration, irrigation, and drainage (Figure 13). Over the 10 weeks of the experiment, the apple tree consumed a depth-equivalent of 173 mm of water. During the same period, some 170 mm of irrigation was added to the root zone to replenish that water being taken up by the tree. We calculate the

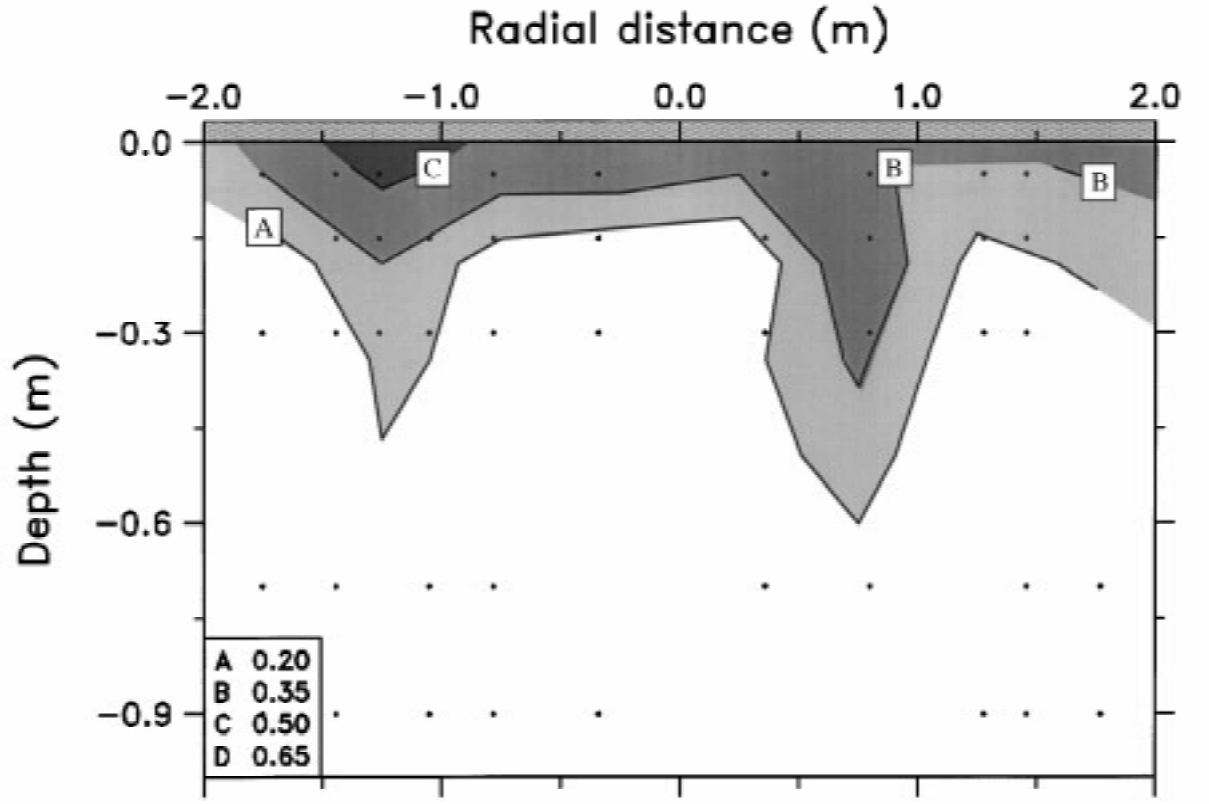

Figure 10. Measurement by TDR of the spatial pattern of the average water uptake, $\Delta\theta$ (% per day) by the covered tree during the period between DOY 90 and 102, which followed a full irrigation of some 50 mm to both sides of the tree on DOY 88. Irrigation is indicated by the shaded region at the soil surface.

cumulative drainage out of the root zone to be some 24 mm. Most of this drainage we believe occurred in the first 10 or so days of the experiment, when the root zone was uniformly wet (Figure 12), especially in the fine sand layer down to 0.6 m. The model results help to explain the early discrepancy between water uptake measured by the TDR, and tree transpiration measured by heat-pulse (Figure 4). Irrespective, the drainage component is small, in our case of zero rainfall, compared to the 'inputs' of irrigation and the 'outputs' of transpiration. This is good for protection of the underlying water bodies, as the actively growing tree had consumed virtually all the applied water in this experimental setup. This highlights the ability of well-timed irrigation being environmentally sustainable.

Discussion

The aim of this experiment was to better understand the root zone dynamics of water uptake by mature apple trees in relation to the spatial distribution of soil water, and of the fine roots. Our goal was to observe how root function is related to root form. This work was also prompted by a desire to test a simple model of water uptake by orchard trees. We also used a plant-based assessment of sap flow to examine how uptake by individual apple roots is related to the total transpirational demand imposed on the plants, and whether individual roots can alter their uptake capacity in response to local changes in soil water availability. This facet of the experiment was prompted by an apparent discord between our measurements in other woody stemmed species, and those of Cabibel and Do (1991). Unlike us, they found that roots of drip-irrigated apple that happened to be in dry soil could have their peak flows at night when transpiration rates were negligible.

Again, our results show the diurnal course of sap flow in the apple roots to be in concert with transpiration measured by sap flow in the tree trunk. Similar observations of such proportional root sap flow have been reported in kiwifruit vines (Green and Clothier,

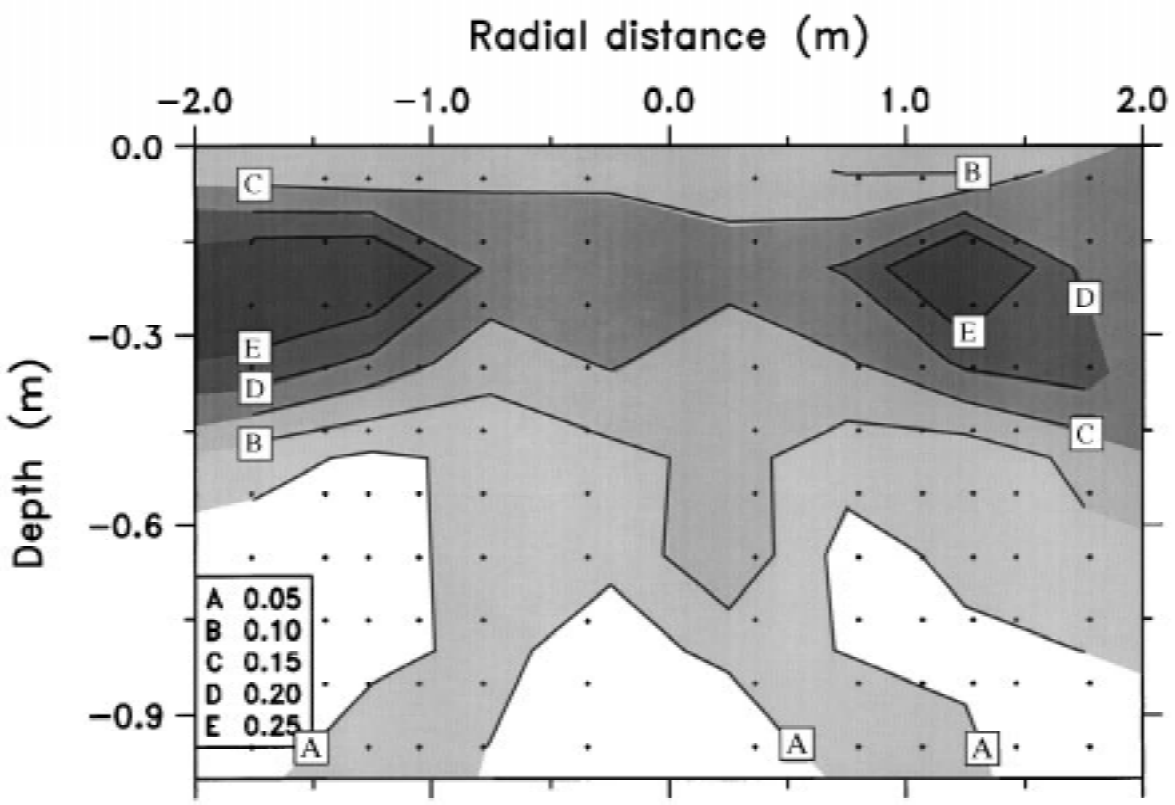

Figure 11. Measurement by root coring of the spatial pattern of root-length density, ρ_L (length of root per unit volume, m m^{-3}), in the root zone of the covered tree. The mid-point of each soil sample is shown by (●).

1995), olive trees (Moreno et al., 1996), grevillea trees (Lott et al., 1996) and eucalyptus trees (Lightbody et al., 1994). We are thus drawn to the conclusion that apple roots normally behave in a similar manner to those of other woody stemmed species. As commented already, this finding differs from that of Cabibel and Do (1991) who reported significant night-time sap flow in small apple roots that were in very dry soil. They attributed this nocturnal flow to a recharge of the trees capacitance. In our experiment we could find no evidence of such nighttime peaks in either of our apple roots. Although some night time flow was recorded, it was always much less than the corresponding sap flow during the middle part of the day and it always coincided with a small nocturnal sap flow in the tree trunk.

The most likely reason for the contrast between our results in apple roots and those of Cabibel and Do (1991) is that our apple tree was well watered. There was probably sufficient water in the root zone to maintain a favorable tree water status so that the trees capacitance was unlikely to have been strongly depleted during the day. Thus, our nighttime sap flow, albeit minor, would be more indicative of transpiration and less due to a recharge of the trees' capacitance. This contention is supported by our independent calculations of transpiration. These show little sap flow and hence little transpiration at night. For water stressed trees we might expect much larger rates of sap flow in the trunks at night as the trees' capacitance is recharged (Caspari et al., 1993). The difference between our measurements, and those of Cabibel and Do (1991), provides further evidence that both the water status of the soil and of the plant have an important influence on the rates of water uptake by individual tree roots.

In our experiment, a differential irrigation was applied to the root system, and this induced an almost instantaneous increased in sap flow in the wetted root (Figures 5 and 6). Similar rapid responses by 'drought stressed' trees to irrigation have been demonstrated by Cermak (1993), Moreno et al. (1996) and others. Cermak (1993) studied sap flow in large beech trees

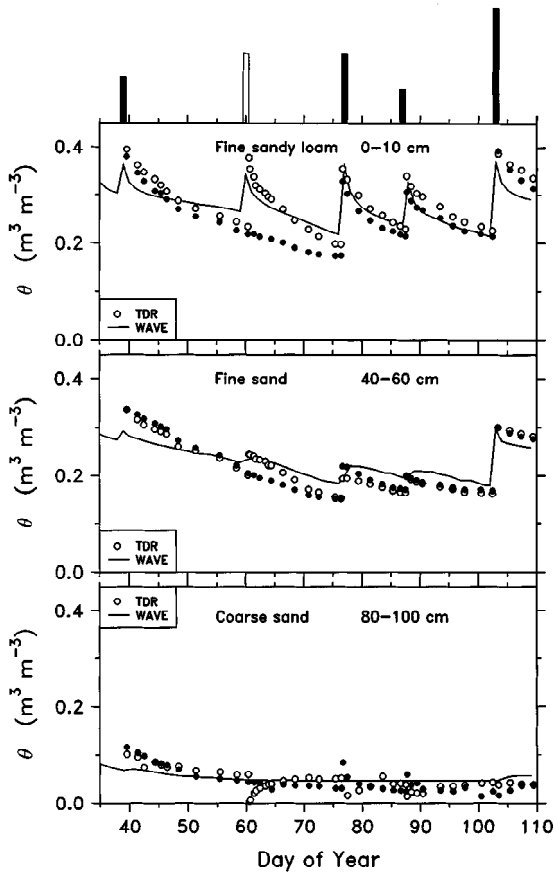

Figure 12. Comparison between measured (symbols) and modelled (dotted line) soil water content. The histograms represent controlled irrigations of between 20 and 70 mm of water. TDR data are from the east (●) and west (○) sides of the root zone.

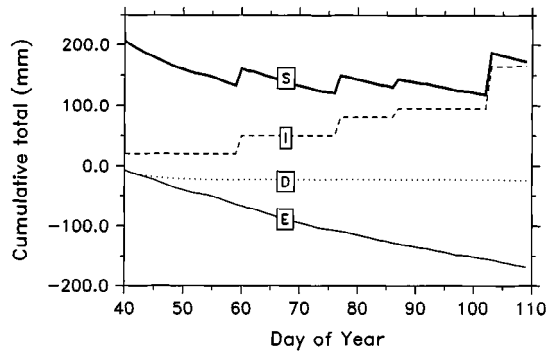

Figure 13. Root-zone water balance: S [mm] is the total amount of water stored in the top 1.0 m, E [mm] is the cumulative transpiration, I [mm] is the cumulative irrigation and D [mm] is the cumulative drainage.

and found a well irrigated tree to have only a slight increase in transpiration following irrigation. Conversely, a severely water-stressed tree demonstrated a 2–5 times increase in sap flow, in a matter of minutes. These water-stressed trees had developed a dense network of fibrous roots in the uppermost soil horizon (0–5 cm), which permitted the trees to utilize effectively any water from irrigation, precipitation or condensation. The well-watered, control trees of their experiment did not possess as many fine roots in the top 0.6 m and consequently showed little response to irrigation. In our apple experiment we saw little evidence of an increase in trunk sap flow following the differential irrigation. There was, however, an increase in measured uptake from a root in the wet part of the root zone and a compensatory decrease in water uptake from a root in the dry part (Figures 4 and 5). Thus, the apple tree was quickly able to alter its pattern of uptake to take advantage of the recently applied irrigation water because there were many fine roots near the soil surface (Figure 11). We have previously observed that kiwifruit (Green and Clothier, 1995) and olive trees (Moreno et al., 1996) can also alter their pattern of water uptake in preference to roots in wet soil.

Unlike the apple roots here, we found in our kiwifruit experiment (Green and Clothier, 1995) only a gradual increase in root uptake activity a few days after irrigation. We attributed this increase to a growth flush of new fine roots. Here, we now see a similar result for one of the apple roots, with the uptake activity gradually increasing after each irrigation. However, the other root showed only a short-term response to irrigation. The enhanced uptake lasted just a day or two. Subsequently, the uptake activity returned back to the level which had existed prior to irrigation. In other words, we see two roots on the same tree locally responding quite differently to similar events of soil wetting (Figure 6). This is similar to the findings of Lott et al. (1996) who observed considerable functional variability among root systems of *Grevillea* trees of similar canopy size. Our observation of a different long-term response for the two roots suggests that there is considerable functional variability across the apple root system.

New measurement techniques are providing improved means by which we can better observe both the changing spatial patterns of water content in the soil and the changing temporal patterns of water uptake by the roots. In particular, Time Domain Reflectometry for measuring soil water content close to roots and

near to the soil surface, in tandem with instantaneous monitoring of sap flow directly within the roots, is providing a sharper picture of how root functioning can change rapidly in response to local changes in the water status of the root zone or patterns of root growth. We feel that progress in understanding the role of roots as the big movers of water and chemicals in soil will, in the near future, continue to remain driven by improvements in our ability to observe the link between distribution of roots and the corresponding uptake patterns (Clothier and Green, 1997). Better observations of the form-function link is key to improving our models of water movement through and beyond the root zone. The measurement-modeling dualism will ultimately improve our ability to predict the fate of any surface applied water and nutrients (De Willingen and Van Noordwijk, 1987).

While we are encouraged by the model results generated by WAVE, we still believe there is much more progress required before we can model effectively the dynamics of water uptake. In particular, we see a need to include aspects of root growth and root turnover. These we can observe from minirhizotron images of fine roots (Clothier and Green, 1997), although the interpretation in terms of a root-length density remains problematic. In terms of functioning, we have observations of root sap flow (Green and Clothier, 1995). These better observations of root form and root function will provide new insights into root system functioning and so rekindle the desire to develop new theories and better models of water movement in the soil.

Acknowledgements

The experimental and analytical research was supported, respectively, by the New Zealand Foundation for Research, Science and Technology under contract No. CO6302 and CO6617. We are grateful to Massey University for contracted usage of the trees in the apple orchard. We acknowledge the technical assistance of Bryan Jardine in building the new heat-pulse instrumentation for the apple roots, and Keith Hughes and David McLeod for their assistance in the root coring.

References

Baker J M and Allmaras R R 1990 System for automating and multiplexing soil moisture measurement by time-domain reflectometry. Soil Sci. Soc. Am. J. 54, 1–6.

Cabibel B and Do F 1991 Mesures thermiques des flux de sève et comportement hydrique des arbres. II. Évolution dans le temps des flux de sève et comportement hydrique des arbres en présence ou non d'une irrigation localisée. Agronomie 11, 757–766.

Caspari H W Green S R and Edwards W R N 1993 Transpiration of well-watered and water-stressed Asian pear trees as determined by lysimetry, heat-pulse, and estimated by a Penman-Monteith model. Agric. For. Meteorol. 67, 13–27.

Cermak J Matyssek R and Kucera J 1993 Rapid response or large, drought-stressed beech trees to irrigation. Tree Physiol. 12, 281–290.

B E Clothier, Scotter D R and Kerr J P 1977 Water retention in soil underlain by a coarse-textured layer: theory and a field application. Soil Sci. 123, 392–399.

Clothier B E and Green S R 1997 Roots: the big movers of water and chemical in soil. Soil Sci. 162, 534–543.

De Willigen P and Van Noordwijk M 1987 Roots, plant production and nutrient use efficiency. Ph.D. thesis, Agricultural University Wageningen.

Feddes R A Kowalik P J and Zaradny H 1978 Simulation of field water use and crop yield. Simul. Monog. PUDOC, Wageningen.

Gardner W 1958 Some steady state solutions of the unsaturated moisture flow equation with application to evaporation from a water table. Soil Sci. 85, 228–232.

Gardner W R 1964 Relation of root distribution to water uptake and availability. Agron. J. 56, 41–56.

Gardner W R 1991 Modelling water uptake by roots. Irrig. Sci. 12, 109–114.

Gerke H H and Van Genuchten M T 1993 A dual-porosity model for simulating the preferential movement of water and solutes in structured porous media. Water Resour. Res. 29, 305–319.

Green S R and Clothier B E 1988 Water use of kiwifruit vines and apple trees by the heat-pulse technique. J. Exp. Bot. 39, 115–123.

Green S R McNaughton K J and Clothier B E 1989 Observations of night-time water use in kiwifruit vines and apple trees. Agric. For. Meteorol. 48, 251–261.

Green S R and Clothier B E 1995 Root water uptake by kiwifruit vines following partial wetting of the root zone. Plant Soil 173, 317–328.

Green S R 1993 Radiation balance, transpiration and photosynthesis of an isolated tree. Agric. For. Meteorol. 64, 201–221.

Green S R and McNaughton K G 1997 Modelling effective stomatal resistance for calculating transpiration from an apple tree. Agric. For. Meteorol. 83, 1–26.

Green S R Clothier B E and McLoud D J 1997 The response of sap flow in apple roots to localised irrigation. Agric. Water Manage. 33, 63–78.

Hughes K A and Gandar P W 1993 Length densities, occupancies and weights of apple root systems. Plant Soil 148, 211–221.

Jarvis P G and McNaughton K G 1986 Stomatal control of transpiration: scaling up from leaf to region. Adv. Ecol. Res. 15, 1–49.

Kerr J P and Clothier B E 1974 Modelling evapotranspiration of a maize crop. Agron. Soc. N.Z. Proc. 5, 49–53.

Landsberg J J and Powell D B B 1973 Surface exchange characteristics of leaves subject to mutual clustering. Agric. Meteorol. 13, 169–184.

Lightbody K E Savage M J and Graham A D N 1994 In situ measurement of sap flow rate in lateral roots and stems of Eucalyptus grandus, under conditions of marginality, using a steady state heat balance technique. J. S. Afr. Hort. Soc. 4, 1–7.

Lott J E Khan A A H Ong C K and Black C R 1996 Sap flow measurements of lateral tree roots in agroforestry systems. Tree Physiol. 16, 995–1001.

Molz F J 1981 Models of water transport in the soil-plant system: A review. Water Resour. Res. 17, 1245–1260.

Moreno F Fernandez J E Clothier B E and Green S R 1996 Transpiration and root water uptake by Olive trees. Plant Soil 184, 85–96.

Mualem Y 1974 A conceptual model of hysteresis. Water Resour. Res. 10, 514–520.

Sinclair T R Murphy C E and Knoerr K R 1976 Development and evaluation of simplified models for simulating canopy photosynthesis and transpiration. J. Appl. Ecol. 13, 813–829.

Swanson R H and Whitfield D W A 1981 A numerical analysis of heat-pulse velocity theory and practise. J. Exp. Bot. 32, 221–239.

Thorpe M R Warrit B and Landsberg J J 1980 Response of apple leaf stomata: a model for single leaves and a whole canopy. Plant Cell Environ. 3, 23–27.

Topp G C Davis J L and Annan A P 1980 Electromagnetic determination of soil water content: Measurements in coaxial transmission lines. Water Resour. Res. 16, 574–582.

Van Genuchten M T 1980 A closed-form equation for predicting the hydraulic conductivity of soil. Soil Sci. Soc. Am. J. 44, 892–898.

Vanclooster M Viaene P Diels J and Feyen J 1995 A deterministic evaluation analysis applied to an integrated soil-crop model. Ecol. Model. 81, 183–195.

Vogeler I Clothier B E and Green S R 1997 TDR estimation of the resident concentration of electrolyte in the soil solution. Aust. J. Soil. Res. 35, 515–526.

Welbank P J and Williams E D 1968 Root growth of a barley crop estimated by sampling with portable powered soil-coring equipment. J. Appl. Ecol. 5, 477–481.

Section Editor: H Lambers